

Experimental realization of a fetching algorithm in a 7 qubit NMR quantum computer

Gui Lu Long^{1,2,3,4} and Li Xiao^{1,2}

¹ *Department of Physics, Tsinghua University, Beijing 100084, China*

² *Key Laboratory For Quantum Information and Measurements, Beijing 100084, China*

³ *Center for Atomic and Molecular Nanosciences, Tsinghua University, Beijing 100084, China*

⁴ *Institute of Theoretical Physics, Chinese Academy of Sciences, Beijing 100080, China*

(November 10, 2018)

Searching for marked items from an unsorted database is an important scientific problem and a benchmark for computing devices as well. Using a 7-qubit liquid NMR quantum computer, we have demonstrated successfully an hybrid quantum fetching algorithm that finds marked items using only a single query. The essential idea is the operation of quantum computers in parallel. We gave the detailed pulse sequence for coherent control of the 7 qubits. The pulse sequence demonstrated here is not only useful for ensemble quantum computation, but also can be regarded as a general purpose control-gate which is useful for experimental design of quantum algorithms and general quantum information processing task in other quantum computer schemes. A generalization of the algorithm that is scalable to arbitrary qubit number is also provided.

The perspective enormous power of quantum computers(QCs) has sparked intensive efforts worldwide. Various schemes have been put forward. Liquid NMR [1–4], quantum dot [5], cavity quantum electrodynamics(QED) [6], linear ion trap [7], superconducting qubit [8], solid-state NMR [9–11] are just a few examples in this long list. By the way they measure, they can be put into two main categories: single qubit-measurement quantum computer (SQC), and ensemble qubit-measurement quantum computer(EQC). Typical examples are Kane’s proposed silicon quantum computer(SQC), and the liquid NMR(EQC). SQC is the ideal system for quantum computation. EQC is in fact an ensemble of many SQC copies. The control and measurement in EQC, such as liquid NMR, is easier than SQC for existing technology. Thus it advances farther in demonstrating quantum information processing such as Deutsch-Josza [12–15], quantum search and counting [16–19], order-finding [20], quantum Fourier transformation [21,22], Shor’s factorization [23], quantum error correction code [24], dense coding [25], and GHZ-state preparation [26].

Usually an ensemble is in a mixed state. Effective pure state(EPS) technique is employed [1–4] to prepare the system so that the ensemble behaves like a pure state. In liquid NMR, a measure that indicates to what extent the system is close to a pure state is the polarization ϵ [4]. If the polarization is equal to 1, the ensemble becomes a pure state ensemble, EQC is equivalent to SQC. By increasing the magnetic field or employing polarization transfer [27,28], polarization can be increased. At present, NMR-QC is operating at a regime with $\epsilon \sim 10^{-5}$. Liquid NMR QC may be used to investigate the behaviour on representative systems and study problems that will be encountered in future scalable technologies.

Redundancy in EQC not only makes qubit control and measurement easy, but also provides source of additional computing power. Madi, Brüschweiler and Ernst [29] put forward Liouville space quantum computation(L-QC). In this mode, the quantum parallelism and the classical parallelism in an ensemble are exploited, and it can achieve exponential speedup for certain problems which are impossible in a pure quantum computer. Different from EPS where all the sub-ensembles are made into the same state as much as possible, L-QC exploits the diversity of states of constituent molecules in an ensemble. Notably, unsorted database search can be exponentially fast in L-QC. Unsorted database search is a benchmark problem for computing devices. It is a mathematical NP-hard problem and plays an important role in computational complexity theory. It is widely used in science and technology, for instance it can break DES-like encryption schemes [31]. To find a marked item from a database with N -items, it requires about $N/2$ queries in a classical computer. In a quantum computer, Grover’s algorithm [32] uses $O(\sqrt{N})$ steps, though a significant square-root speedup but still exponentially slow. When searching a database with unknown number of marked items, an estimate of the number of marked states is required because it depends sensitively on this number. Furthermore it has been shown that Grover’s algorithm is optimal for quantum computers [30,33,34]. This optimality restriction can only be broken off from outside of quantum computer and it has been achieved by Brüschweiler in L-QC [35]. Brüschweiler’s algorithm requires only $\log_2 N$ search steps. For instance, to decipher a DES code, it is equivalent to find a marked item from a database with $N = 2^{56} \simeq 10^{17}$ items. A quantum computer running Grover’s algorithm requires about $0.8 \times 2^{28} \simeq 2 \times 10^8$ steps, whereas Brüschweiler’s algorithm requires only 56 search steps. Recently, it is found that L-QC computing can achieve the absolute maximum in unsorted database search, a single query suffices to find every marked item using a hybrid quantum fetching algorithm [36].

In this paper, we report the experimental implementation of this hybrid quantum fetching algorithm in a NMR system with 7 qubits. The implementation requires coherent quantum control of all the 7 qubits. Pulse sequences for the quantum gate operations are given explicitly. We also scale up the algorithm to arbitrary qubit number which can be used in scalable ensemble quantum computer. In particular, we found that the algorithm can be implemented directly from thermal equilibrium.

Here we briefly introduce the fetching algorithm, details can be found in Ref. [36]. In operator-product formalism, a pure-state $|\phi_m\rangle$ is represented by direct product of the polarization operators [29], $|\phi_m\rangle = |\alpha\alpha\beta\ldots\alpha\beta\rangle \iff \rho_m = I_1^\alpha I_2^\alpha I_3^\beta \ldots I_{n-1}^\alpha I_n^\beta$ where $|\alpha\rangle, |\beta\rangle$ are the spin up and down eigenstates of I_z , the Pauli spin operator respectively.

The one-qubit state $|\alpha\rangle$ and $|\beta\rangle$ can be expressed in terms of the polarization operator, namely $2I^\alpha = 2|\alpha\rangle\langle\alpha| = (\mathbf{1} + 2I_z)$, $2I^\beta = 2|\beta\rangle\langle\beta| = (\mathbf{1} - 2I_z)$. In L-QC with 7-qubit, one qubit is used as ancilla as required by L-QC, the other six qubits represent a database with $2^6 = 64$ items, namely $|0\rangle = |000000\rangle$, $|1\rangle = |000001\rangle$, ..., $|63\rangle = |111111\rangle$. To start, the L-QC system is prepared in a mixed state, apart from a scaling factor

$$\rho_0 = I_0^\alpha = |0,0\rangle\langle 0,0| + |0,1\rangle\langle 0,1| + \dots + |0,i\rangle\langle 0,i| + \dots + |0,63\rangle\langle 0,63|, \quad (1)$$

where we have written the ancilla qubit state explicitly for clarity, namely $|0000000\rangle = |0,0\rangle$. Then the query function f is applied to the system, which changes state (1) into

$$\rho_1 = |f(0),0\rangle\langle f(0),0| + \dots + |f(i),i\rangle\langle f(i),i| + \dots + |f(63),63\rangle\langle f(63),63|. \quad (2)$$

For constituent (to distinguish pure state from mixed state, we call a part in a pure state as component, and a part in a mixed state as constituent) corresponding basis i , query function does nothing to it if i does not satisfy the query, otherwise it flips the ancilla qubit. After the implementation of query, a read-out pulse is applied to the ancilla qubit and its spectrum is measured. Those constituents that satisfy the query have their ancilla qubit flipped, and on the ancilla qubit spectrum, the peaks corresponding to these constituents will have their peaks inverted. The item that a peak corresponds is determined by the peak frequency. Then by looking at the ancilla qubit spectrum, one can easily read out the marked items.

The experiment is carried out on a VARIANT INOVA-600MHz spectrometer. The liquid sample is ^{13}C labeled crotonic acid with formula $\text{C}^1\text{H}_3\text{C}^2\text{H}^1 = \text{C}^3\text{H}^2\text{C}^4\text{O}_2\text{H}$, which is manufactured by Cambridge Isotope Laboratories Inc. The same substance has been used in Ref. [26] to prepare GHZ state. The chemical structure and the J couplings can be found in Fig.2 of Ref. [26]. The seven qubits are the four carbon nuclear spins, two proton spins in the middle connected with the middle two carbon. The 3 methyl proton spins (denoted M) have the same chemical shift, and they are treated as a single qubit. The sample is firstly dissolved in a 0.5 ml acetone and then injected into a 5 mm tube, deaired and sealed. The ancilla qubit is chosen as C^2 . Nuclear spins of H^1 , C^3 , C^1 , H^3 , C^4 and H^2 are assigned as qubit 1, 2, 3, 4, 5 and 6 respectively, in decreasing order by the J magnitude of respective nuclear spin with the ancilla bit. Our measured J values agree very well with that in Ref. [26]. The J_{0i} coupling between qubit 0 and the rest six qubits are (in Hz): 156.0, 69.7, 41.6, -7.1 , 1.4, -0.7 for i from 1 to 6 respectively. If J_{0i} is positive such as qubit 1, 2, 3 and 5, we assign $|\alpha\rangle = |0\rangle$ and $|\beta\rangle = |1\rangle$, and if J_{0i} is negative such as qubit 4 and 6, we assign $|\alpha\rangle = |1\rangle$ and $|\beta\rangle = |0\rangle$. In doing so, the peaks in the ancilla qubit spectrum will represent numbers monotonically in increasing order starting from $|000000\rangle$ with frequency $\omega_0 + \sum_{i=1}^6 \pi|J_{0i}|$ on the far left to $|111111\rangle$ with frequency $\omega_0 - \sum_{i=1}^6 \pi|J_{0i}|$ on the far right.

The query function f is important in unsorted database search. It is treated as a blackbox [35,37,38]. The query blackbox used in this work is given in Fig.1a. It checks whether an item's first 3 bits values are 100. The H-gate in the figure is a Hadamard-like gate with the expression

$$\text{H}^0 = \exp(-i\pi I_x^0) \exp(-i\frac{\pi}{2} I_y^0) = \frac{i}{\sqrt{2}} \begin{pmatrix} 1 & 1 \\ 1 & -1 \end{pmatrix}. \quad (3)$$

It is realized using NMR pulse sequence $R_x^0(\pi)R_y^0(\frac{\pi}{2})$. The superscript(subscript) is the qubit(direction) on which the pulse is applied. The triple-qubit controlled phase rotation in the query is explicitly as

$$R_z^{\text{ccc}}(\pi) = \exp(-i\pi I_z^0 \frac{(1-2I_z^1)}{2} \frac{(1+2I_z^2)}{2} \frac{(1+2I_z^3)}{2}). \quad (4)$$

It is clear that when the first three qubits are in values 1, 0 and 0 respectively, the expression $\frac{(1-2I_z^1)}{2} \frac{(1+2I_z^2)}{2} \frac{(1+2I_z^3)}{2}$ gives an identity operator, and the whole expression in (4) becomes a rotation about the z -axis through π . Otherwise, one or more of the factors becomes zero, and Eq.(4) reduces to an identity operator. This implements the triple-qubit controlled phase rotation. Further it can be reduced to basic one- and two-qubit gates by the recursive formula

$$\exp(-i\lambda 2^n I_{k_1 z} I_{k_2 z} \dots I_{k_n z} I_{k_{n+1} z}) = V_n \exp(-i\lambda 2^{n-1} I_{k_1 z} \dots I_{k_{n-1} z} I_{k_{n+1} z}) V_n^+, \quad (n \geq 2) \quad (5)$$

given in Refs. [39], where

$$V_n = \exp(-i\frac{\pi}{2} I_{k_{n+1} x}) \exp(-i\pi I_{k_n z} I_{k_{n+1} z}) \exp(i\frac{\pi}{2} I_{k_{n+1} x}) \exp(-i\frac{\pi}{2} I_{k_{n+1} y}). \quad (6)$$

The whole pulse sequence is drawn in Fig.2. It involves the coherent control of all the 7 qubits. It consists of 47 spin-selective radio frequency pulses, together with several free evolution intervals. The decoupling is implemented using the compound decoupling pulse sequence WALTZ16 [40]. The total duration of the pulse sequence is about 90 ms which is well within the system's 2s decoherence time (T_2) [26].

We actually implemented the algorithm directly on the thermal equilibrium state without preparing I_0^α . In thermal equilibrium, the density operator is

$$\rho \simeq \frac{1}{N} (\mathbf{I} - \beta H) = \frac{1}{N} \left(\mathbf{I} - \beta \sum_{i=0}^{n-1} \gamma_i B \sigma_z^i \right). \quad (7)$$

The state we need is $I_0^\alpha = (I + \sigma_z^0) \sim \sigma_z^0$ and can be written as $\rho' = \frac{1}{N} (I - \beta \gamma_0 B \sigma_z^0)$, apart from an identity operator and a scaling factor. γ_i is the gyromagnetic ratio of qubit i , and $\beta = 1/kT$. After the implementation of query, only the ancilla qubit state is changed,

$$U_f \rho' U_f^\dagger = \frac{1}{N} \left(I - \beta U_f \gamma_0 \sigma_z^0 U_f^\dagger - \beta \sum_{i=1}^{n-1} \gamma_i B \sigma_z^i \right). \quad (8)$$

Upon measurement, a selective read-out pulse is applied to the ancilla qubit, the first and last terms in eq.(8) do not contribute to the signal. The signal we acquire is only from the second term which is the one we need. Thus we can perform the algorithm directly from thermal equilibrium. Shown at the top of Fig.3 is the ancilla qubit spectrum at the thermal equilibrium state. It represents the unsorted database. The spectrum is divided into 8 major groups, and each group contains 4 peaks where two inner peaks are about 3 times as high as the outer two short peaks. This is because qubit 4 is composed of 3 identical proton spins, and they produce 4 energy levels and thus make 4 modulations on the ancilla bit spectrum with modulation frequency $3J_{04}$ (all three spins up), J_{04} (two spins up and one spin down, triply degenerate), $-J_{04}$ (two spins down and one spin up, triply degenerate), and $-4J_{04}$ (all three spins down). Because the multiplicity of levels due to qubit 4, the number of peaks in spectrum is doubled. Thus within each group the left two peaks (one short and one tall) corresponds to qubit 4 at state 0, and the right two peaks corresponds to qubit 4 at state 1. While the doubling of levels gives additional work in preparing an effective pure state in EPS QC, it is advantageous for L-QC because this peak-doubling makes the identification of peak inversion a lot easier. Within each peak in Fig.3, there are still 4 finer peaks due to the different states of qubit 5 and 6. In finer frequency resolution, they are clearly separated and visible. All the 128 peaks in the spectrum correspond items from 0 at the far left and 63 at the far right. It is interesting to notice the separation of the major groups. Counting from left, the distance between group 2 and 3, 6 and 7 are shorter than that between groups 1 and 2, 3 and 4, 5 and 6, 7 and 8. The distance between 4 and 5 is the largest. These distance differences can be easily understood from the J parameter magnitude. The centroid positions of these peaks are of the form $\pm |J_{01}| \pm |J_{02}| \pm |J_{03}|$.

Shown in bottom of Fig.3 is the ancilla bit spectrum after the implementation of the query. The spectrum is a result with only 8 scans. Shown in the middle of Fig.3 is part of the spectrum after the query, here it is clearly shown that there are 4 peaks within each peak. Even with this small scan number, it is clearly visible from the figure that the peaks in the fifth group have their peaks inverted. The doubling of peaks due to qubit 4 makes the identification of peak inversion easier, in particular by looking at the inner tall peaks. They correspond to items from 100000 to 100111 which are the items that we are searching. As compared with that before the query, the height of peak is reduced. This is due to the decoherence that occurs during the computation. The result is striking because no measures have taken to compensate the decoherence. The fetching of the marked states is successfully demonstrated.

It is worth pointing that the algorithm demonstrated here is in fact the parallel operation of quantum computers. The capability of doing quantum computing in parallel lies in the unitarity nature of QC operations. A function f in a QC is carried out by a unitary transformation U_f which corresponds to a sequence of radio frequency pulses and free evolutions. This pulse sequence evaluates the function value for $|00\dots 0\rangle$, and the same pulse sequence also evaluates the function value of $|11\dots 1\rangle$ and any other inputs! When applied to a superposition of basis states, it evaluates the function values of all the basis states! When applied to an ensemble in mixed state, the pulse sequence transforms each constituent sub-ensemble of basis states into their corresponding function values. The pulse sequence is ubiquitous to all molecules in the ensemble and acts as a super-commander to all the basis states. Each basis state goes through the transformation required by the specific function irrespective of its surroundings: alone, or lined up hand by hand with other basis states in a superposed pure state, or scattered here and there in different sub-ensembles in a mixed state.

The algorithm can be scaled up to systems with arbitrary n qubit system. An example for the query network for n -qubit system is shown in Fig.1b. The multiple-qubit($i_1 i_2 \dots i_n$) controlled phase rotation can be written explicitly

$$R_z^{c^n}(\pi) = \exp(-i \frac{\pi}{2^n} I_z^0 (1 + s_1 (-1)^{i_1} 2I_z^1) \dots (1 + s_{n-1} (-1)^{i_{n-1}} 2I_z^{n-1}) (1 + s_n (-1)^{i_n} 2I_z^n)), \quad (9)$$

where s_i denotes the sign of J_{0i} . Using formulas (5) and (6), it can be decomposed into basic one- and two- qubit gate operations. They might be used in other ensemble quantum computers, such as the proposed schemes in Refs. [10,11].

To summarize, we have implemented a hybrid quantum fetching algorithm in a 7 qubit NMR quantum computer. The algorithm is essentially the parallel operation of quantum computers. A scale-up version of the algorithm is provided. Furthermore it is demonstrated that the algorithm can be implemented in a thermal equilibrium state directly.

The authors are grateful for help from Prof. X. Z. Zeng, M. L. Liu, J. Luo for Help. This work is supported in part by China National Science Foundation, the National Fundamental Research Program, Contract No. 001CB309308 and the Hang-Tian Science foundation.

- [1] D. G. Cory, A. F. Fahmy, and T. F. Havel, *PNAS* **94**, 1634(1997).
- [2] N. A. Gershenfeld and I. L. Chuang, *Science* **275**, 350 (1997).
- [3] I. L. Chuang et. al., *Proc. Roy. Soc. LondA*, **454**, 447(1998).
- [4] E. Knill, I. L. Chuang, and R. Laflamme, *Phys. Rev.* **A57**, 3348(1998).
- [5] D. Loss and D.P. DiVincenzo, *Phys. Rev.* **A57**, 120 (1998).
- [6] J. Sledtor, H. F. Weinfurter, *Phys. Rev. Lett.*, **74**, 408(1995).
- [7] S. I. Cirac, P. Zoller, *Phys. Rev. Lett.*, **74**, 4019(1994)
- [8] Yu Makhlin, G. Schön, and A. Shnirman, *Rev. Mod. Phys.* **68**, 733 (1997).
- [9] B. E. Kane, *Nature* **393**, 133-136 (1998).
- [10] F. Yamaguchi and Y. Yamamoto, *Microelectron. Eng.* **47**, 273 (1999).
- [11] T. D. Ladd et. al., *Phys. Rev. Lett.* **89**, 017901 (2002).
- [12] I.L. Chuang et. al., *Nature* **393**, 143 (1998).
- [13] N. Linden, H. Barjat and R. Freeman, *Chem. Phys. Lett.* **296**, 61 (1998).
- [14] K. Dorai, Arvind and A. Kumar, *Phys. Rev. A* **6104**, 2306 (2000).
- [15] R. Marx et. al., *Phys. Rev. A* **62**, 012310 (2000).
- [16] I.L. Chuang, N. Gershenfeld and M. Kubinec, *Phys. Rev. Lett.* **80**, 3408 (1998).
- [17] J.A. Jones, M. Mosca and R. H. Hansen, *Nature* **393**, 344 (1998).
- [18] L.M.K. Vandersypen et al., *Appl. Phys. Lett.* **76**, 646 (2000).
- [19] G. L. Long et. al., *Phys. Lett.* **A286**, 121(2001).
- [20] L.M.K. Vandersypen et. al., *Phys. Rev. Lett.* **85**, 5452(2000).
- [21] Liping Fu, Jun Luo, Li Xiao, Xizhi Zeng, *quant-ph/9905058*.
- [22] Y.S. Weinstein et. al., *Phys. Rev. Lett.* **86** 1889 (2001). Also available as eprint *quant-ph/9906059*.
- [23] L.M.K. Vandersypen et. al., *Nature* **414**, 883 (2001).
- [24] E. Knill et. al., *Phys. Rev. Lett.* **86**, 5811 (2001).
- [25] X. M. Fang et. al., *Phys. Rev.* **A61**,. 022307(2000).
- [26] E. Knill, R. Laflamme, R. Martinez, and C. H. Tseng, *Nature*, **404**, 368 (2000).
- [27] A. S. Verhulst et. al., *Appl. Phys. Lett.*, **79**, 2480(2001).
- [28] J. Luo and X. Z. Zeng, *quant-ph/9811044*.
- [29] Z. L. Madi, R. Bruschweiler, R. R. Ernst, *J. Chem. Phys.*, **109**, 10603, (1998)
- [30] C. H. Bennett et. al., *SIAM J. Comput.* **26**, 1510 (1997).
- [31] Brassard G., *Science* **275**, 627 - 628 (1997).
- [32] L. K. Grover, *Phys. Rev. Lett.*, **79**, 325(1997).
- [33] M. Boyer, G. Brassard, P. Hoyer, and A. Tapp, *Fortschr. Phys.* **46**, 493 (1998).
- [34] Ch. Zalka, *Phys. Rev.* **A60**, 2746 - 2751 (1999).
- [35] R. Bruschweiler, *Phys. Rev. Lett.*, **85**, 4815 (2000).
- [36] L. Xiao and G. L. Long, *quant-ph/0112162*.
- [37] D. Biron et. al., *quant-ph/9801066*.
- [38] L. Xiao, G. L. Long, H. Y. Yan, and Y. Sun, *J. Chem. Phys.* **117**, No. 8 (2002).
- [39] X. Miao, *Mol. Phys.*, **98**, 625 (2000), and in *quant-ph/0003068*.
- [40] A.J. Shaka, J. Keeler. R. Freeman. *J. Magn. Reson.* **53**. 313 (1983)

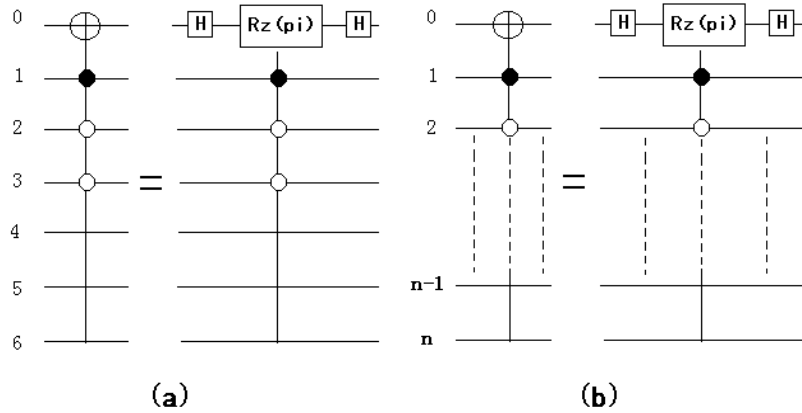


FIG. 1. Quantum network for query: (a) used in this work; (b) in arbitrary qubit number system. H is a Hadamard-like transformation. A solid dot at the intersection with a qubit line means 1, and circle means 0. $R_z(\pi)$ is a π rotation about the z -axis.

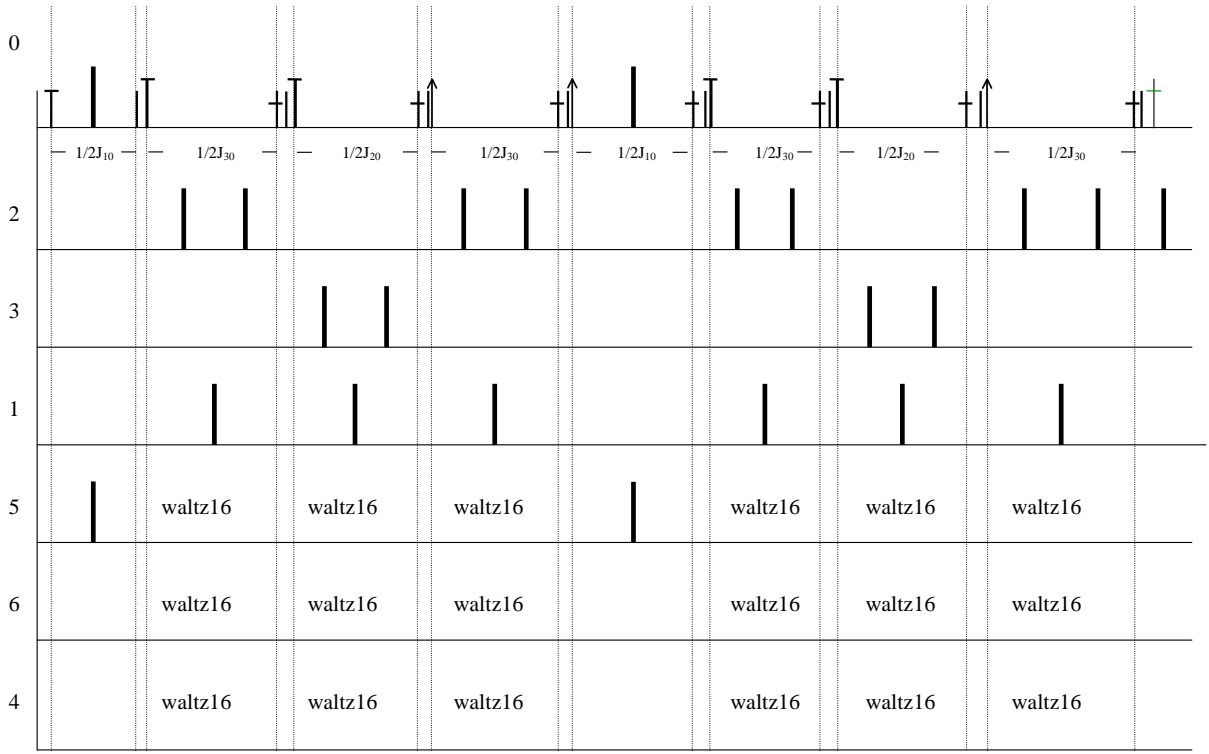


FIG. 2. The pulse sequence for the fetching algorithm. The symbols(in brackets with sub-total number) for different pulses (in degrees) are: 180 along y (thick long line, 23), 90 along y (thin short line with a bar at top,1), 90 along $-y$ (thin short line with a bar at middle, 7), 112.5 along y (thin long line with bar at top, 4), 22.5 along $-y$ (thin long line with bar at middle, 1), 67.5 along y (thin long line with arrow, 3) and 90 along x (thin short line, 8).

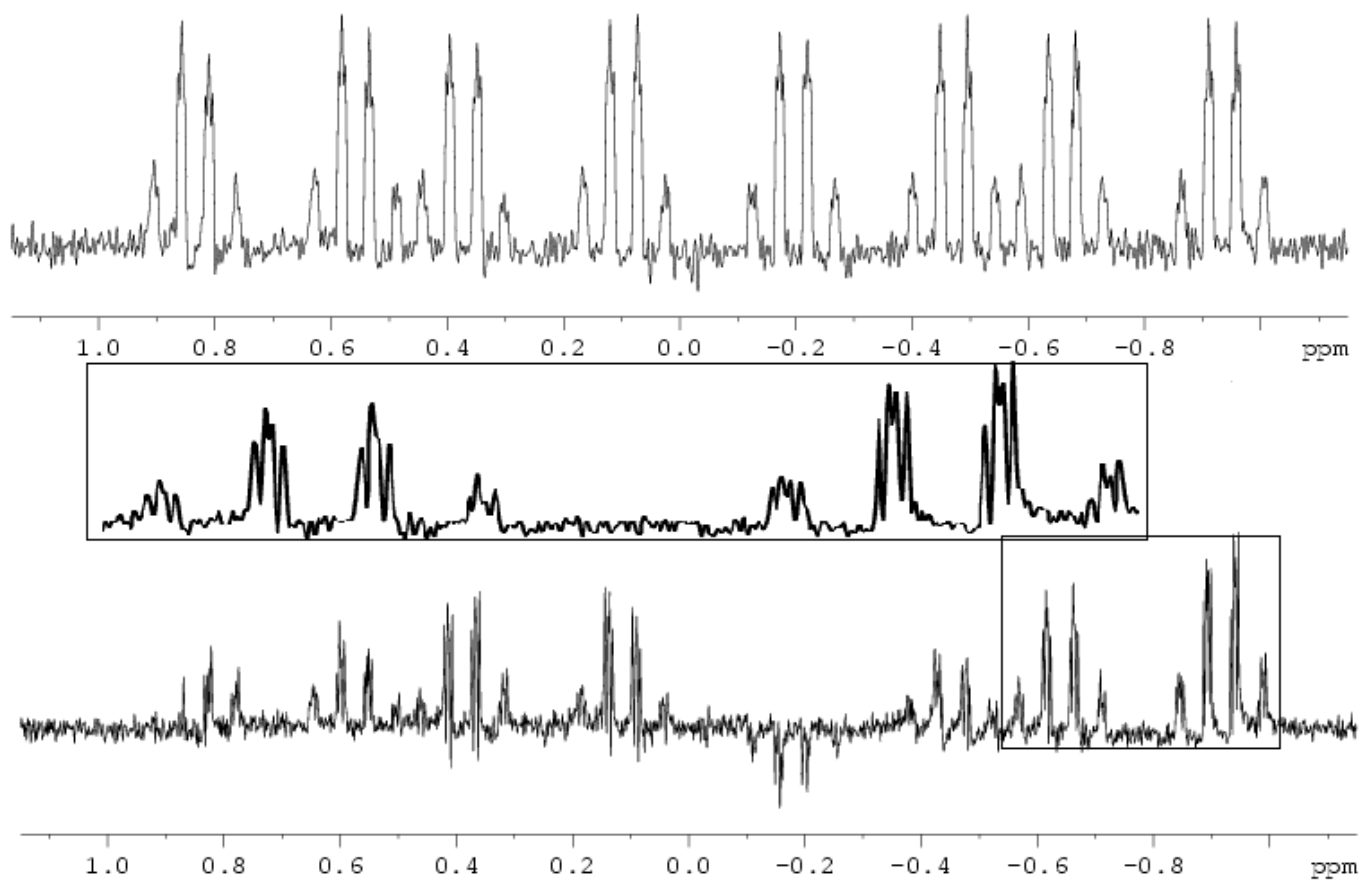


FIG. 3. The spectra before(top) and after(bottom) the implementation of query. The plot in the middle is a part of the spectrum boxed at the bottom. Here it is seen that each peak in the bottom spectrum has 4 sub-peaks.